Neurobiology of Disease 173 (2022) 105854

Contents lists available at ScienceDirect

Neurobiology of Disease

journal homepage: www.elsevier.com/locate/ynbdi

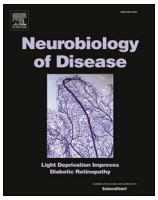

Postnatal Foxp2 regulates early psychiatric-like phenotypes and associated molecular alterations in the R6/1 transgenic mouse model of Huntington's disease

Ened Rodríguez-Urgellés [a,b,c], Irene Rodríguez-Navarro [a,b,c], Iván Ballasch [a,b,c], Daniel del Toro [a,b,c], Ignacio del Castillo [a,b,c], Verónica Brito [a,b,c], Jordi Alberch [a,b,c,d,*], Albert Giralt [a,b,c,d,*]

[a] Departament de Biomedicina, Facultat de Medicina, Institut de Neurociències, Universitat de Barcelona, Barcelona, Spain
[b] Institut d'Investigacions Biomèdiques August Pi i Sunyer (IDIBAPS), Barcelona, Spain
[c] Centro de Investigación Biomédica en Red sobre Enfermedades Neurodegenerativas (CIBERNED), Spain
[d] Production and Validation Center of Advanced Therapies (Creatio), Faculty of Medicine and Health Science, University of Barcelona, 08036 Barcelona, Spain

ARTICLE INFO

Keywords:
Striatum
Adolescent mice
Tor1A
Proteomics
Impulsivity
Hyperactivity
Social skills

ABSTRACT

Huntington's Disease (HD) is a devastating disorder characterized by a triad of motor, psychiatric and cognitive manifestations. Psychiatric and emotional symptoms appear at early stages of the disease which are consistently described by patients and caregivers among the most disabling. Here, we show for the first time that Foxp2 is strongly associated with some psychiatric-like disturbances in the R6/1 mouse model of HD. First, 4-week-old (juvenile) R6/1 mice behavioral phenotype was characterized by an increased impulsive-like behavior and less aggressive-like behavior. In this line, we identified an early striatal downregulation of Foxp2 protein starting as soon as at postnatal day 15 that could explain such deficiencies. Interestingly, the rescue of striatal Foxp2 levels from postnatal stages completely reverted the impulsivity-phenotype and partially the social impairments concomitant with a rescue of dendritic spine pathology. A mass spectrometry study indicated that the rescue of spine loss was associated with an improvement of several altered proteins related with cytoskeleton dynamics. Finally, we reproduced and mimicked the impulsivity and social deficits in wild type mice by reducing their striatal Foxp2 expression from postnatal stages. Overall, these results imply that early postnatal reduction of Foxp2 might contribute to the appearance of some of the early psychiatric symptoms in HD.

1. Introduction

Huntington's Disease (HD) is an autosomal dominant inherited neurodegenerative disorder characterized by a triad of motor, psychiatric and cognitive manifestations (Walker, 2007), caused by a pathological CAG repeat expansions in the human *Huntingtin (HTT)* gene on chromosome 4p16.3 (Gusella et al., 1983; MacDonald, 1993). Medium-spiny projection neurons of the caudate nucleus and putamen (striatum) are the most vulnerable cell types suffering a progressive neurodegeneration, which eventually lead to death (Cepeda et al., 2007). In the early stages, adult-onset HD patients develop personality changes encompassing a wide range of psychiatric and emotional disturbances, which can precede the classical motor symptoms by up to a decade or even more (Epping et al., 2016). Accordingly, HD individuals commonly report progressive apathy, depression, anxiety, irritability, aggression, psychosis, mania, suicidal ideation, disinhibition, impulsivity, risk-taking behavior, obsessive/compulsive behavior, sleep disturbances and unawareness (Nance and Sanders, 1996; Pflanz et al., 1991). Importantly, depression, anxiety, and irritability significantly correlate with increased likelihood of suicidal ideation (McGarry et al., 2019), whereas suicide has been found as the second common cause of death in HD (Solberg et al., 2018). Paradoxically, available treatments are uniquely oriented to alleviate motor symptoms whereas psychiatric disease symptoms are targeted to a lesser extent (Dorsey et al., 2011), even though when several studies have consistently reported that psychiatric disturbances worsen quality of life, possibly, to a greater extent

* Corresponding authors at: Dept. Biomedicina, Facultat de Medicina, Institut de Neurociències, Universitat de Barcelona, C/Casanova 143, Barcelona 08036, Spain.
E-mail addresses: alberch@ub.edu (J. Alberch), albertgiralt@ub.edu (A. Giralt).

https://doi.org/10.1016/j.nbd.2022.105854
Received 6 May 2022; Received in revised form 11 August 2022; Accepted 23 August 2022
Available online 24 August 2022

than motor symptoms of the disease (Ho et al., 2009). HD animal models recapitulate faithfully the motor phenotype observed in humans (Chiu et al., 2011; Renoir et al., 2011) although early and pre-symptomatic psychiatric disturbances are poorly addressed. Concomitant with this lack of knowledge about psychiatric disturbances their underlying molecular mechanisms also remain to be determined.

Dysfunction in the human forkhead box protein P2 (Foxp2) gene could be one of those mechanisms. Foxp2 is a member of the forkhead box family of transcription factors and it has been identified as a relevant genetic risk factor for schizophrenia and other psychiatric features (Sanjuán et al., 2006; Soler Artigas et al., 2020; Tolosa et al., 2010). Accordingly, the *Foxp2* gene has largely been considered as a potential susceptibility locus in neuropsychiatric disorders (Khanzada et al., 2017). Interestingly, some of these psychiatric features related with *FOXP2* common variations resemble to those psychiatric symptoms observed in HD patients, suggesting that changes in Foxp2 levels or function could underlie the psychiatric symptoms in HD. In this line, reduced expression of the Foxp2 protein has been found in late stages of mouse models of HD (Hachigian et al., 2017). However, the role of Foxp2 in the regulation of the early psychiatric symptoms provoked by the mutant huntingtin has not been characterized.

In this work we have analyzed the early dysregulation of Foxp2 from postnatal days in different brain areas, which could be linked to early behavioral and molecular changes in the early stages of R6/1 mouse model. Interestingly, a battery of behavioral tests revealed an early phenotype in 4-week-old (juvenile) R6/1 mice, showing increased impulsive-like behavior and less aggressive-like behavior. Surprisingly, 4-week-old R6/1 compared to age-matched wild type (WT) mice already showed clear structural and functional alterations, such as decreased dendritic spine density and dysregulation of striatal protein expression. As a proof-of-concept, the rescue of striatal Foxp2 levels from postnatal ages reverted impulsivity-phenotype, improved the striatal dendritic pathology and restored striatal protein dysregulation. Also, specific down-regulation of Foxp2 in the striatum of 4-week-old WT mice was sufficient to induce some of the psychiatric-like symptoms resembling to those observed in the 4-week-old R6/1 mice. These results highlight the potential role of Foxp2 in the regulation of very early psychiatric-like symptoms observed in HD.

2. Materials and methods

2.1. Animals

Transgenic R6/1 mice (Mangiarini et al., 1996) expressing the N-terminal exon-1 fragment of m*Htt* containing 115 CAG repeats, were used as a murine model of HD. Heterozygous R6/1 male mice were originally acquired from Jackson Laboratory (Bar Harbor, ME, USA) and maintained in a B6CBA genetic background from mating transgenic male mice (C57BL/6 J x CBA/J) with F1 females. HdhQ7 WT mice with 7 CAG repeats and HdhQ111 knock-in mice (KI), with targeted insertion of 109 CAG repeats that extends the glutamine segment in murine huntingtin to 111 residues, were maintained on a C57BL/6 genetic background. Male and female HdhQ7/Q111 heterozygous mice were intercrossed to generate age-matched HdhQ7/Q111 heterozygous and HdhQ7/Q7 WT littermates (Brito et al., 2014). Genotypes were determined by polymerase chain reaction (PCR) from ear biopsy. Microchips were implanted under the mice skin providing information about their birth, location, and genotype. All mice were housed in numerical birth order in a room kept at 19–22 °C and 40–60% humidity under a 12:12 light/dark cycle with access to water and food *ad libitum*. All experiments were conducted exclusively with male mice to avoid estrus hormonal alterations. WT littermates were used as a control group. Standard animal procedures were approved by the animal experimentation Ethics Committee of the Universitat de Barcelona (274/18) and Generalitat de Catalunya (10/20), in agreement with the Spanish (RD53/2013) and European (2010/63/UE) regulations for the care and use of laboratory animals.

2.2. Open field

The apparatus consisted of a white square arena measuring 40 × 40 × 40 cm in length, width and height. A dimly light intensity of 60 lx was detected throughout the arena. Animals were placed on the arena center and allowed to explore freely for 15 min. Spontaneous locomotor activity was measured. At the end of each trial, defecations were removed, and the apparatus was wiped with water. Animals were tracked and recorded with SMART junior software (Panlab, Spain).

2.3. Elevated plus maze

Briefly, the plus maze was made of plastic and consisted of two opposing 30 × 8 cm open arms, and two opposing 30 × 8 cm arms enclosed by 15 cm-high walls. The maze was raised 50 cm above the floor and lit by dim light. Each mouse was placed in the central square of the maze, facing an open arm and its behavior was scored for 5 min. At the end of each trial any defecation was removed, and the apparatus was wiped with water. We recorded the time spent in the open arms, which normally correlates with low levels of anxiety. Animals were tracked and recorded with SMART junior software (Panlab, Spain).

2.4. Cliff avoidance test

Jumping behavior was performed as previously described(Matsuoka et al., 2005). A round platform (an inverted glass container with a diameter of 13 cm and a height of 20 cm) was in a bench of the room. Mice were placed on the platform and allowed to remain for 15 min. The latency to jump out of the platform was registered and was inferred as a measure of impulsivity.

2.5. Resident-Intruder test

An adapted resident-intruder paradigm was carried out based on previous protocol(Häring et al., 2015). After 4 days of single housing resident-intruder test was performed on the day test. Single housed residents were exposed for 10 min to an unfamiliar similar aged intruder (socially housed). Active social behavior as facial and genital sniffing, and active aggressive behavior as physical struggling were manually registered. Animal tracking were recorded *via* a CCD camera above the arena. Animals were tracked and recorded with SMART junior software (Panlab, Spain).

2.6. Forced swimming test

The forced swimming test was used to evaluate behavioral despair. Animals were subjected to a 6 min trial during which they are forced to swim in an acrylic glass (35 cm height x 20 cm diameters) filled with water, and from which they cannot escape. The time that the test animal spent in the cylinder without making any movements except those required to keep its head above water was measured.

2.7. Viral constructs and stereotaxic injection

For the specific overexpression of Foxp2 in the mice striatum, pups at postnatal day P0-P2 were subjected to bilateral intrastriatal injections. Adeno-associated virus (AAV) expressing Foxp2 under CamKIIα promoter (AAV9-CamKIIa-eGFP-2A-mFoxp2-WPRE, (Vector Biolabs, Pennsylvania, USA) was injected in R6/1 mice (R6/1-Foxp2) and WT mice (WT-Foxp2) and AAV carrying GFP (rAAV5-CamKIIa-eGFP-2A-WPRE, UNC Vector Cre, North Carolina, USA) used as a control was injected in both R6/1 mice (R6/1-GFP) and WT mice (WT-GFP). For the mimicking experiments, wild-type mice at the same age and conditions were used and injected with AAV8-mCherry-U6-Scramble (#1781,

Vector Biolabs) or AAV8-mCherry-U6-mFOXP2-shRNA (#shAAV-259,597, Vector Biosystems). At postnatal day (P0-P2) R6/1 male mice and WT littermates were subjected to stereotaxic surgery through hypothermia-induced anesthesia. Pups were wrapped in Kleenex tissue and immersed in crushed ice up to the neck for 3 min. Hypothermia-induced anesthetized pups were fixed in the stereotaxic apparatus, their heads were cleaned with ethanol 70%. Skin head and skull were gently penetrated by a sterile needle to performed one incision in each brain hemisphere. 300 nl of viral vectors were injected in each incision to bilaterally target the striatum. The following coordinates relative to Lambda (anteroposterior and lateral) and from skull (dorsoventral) were used: AP: +2.4 mm; L: ±1 mm and DV: −1.9 mm. Viral vectors were injected with a 5 μl Hamilton syringe at an infusion rate of 100 nl/min. The needle was left in place for 2 min to ensure complete diffusion of the AAVs. After surgery, pups were warm up for 30 min inside a plastic box filled with breeding and heated underneath by an electric blanket. After fully recovery, pups were returned to their home cage. All mice subjected to surgery that survived and showed no ethical and healthy problems (such as head inclination or > 15% of body weight loss) were also evaluated for behavioral characterization. Once the behavioral characterization was done, half of the brain was used to verify the site of injection by immunofluorescence (see "tissue preparation and immunofluorescence" section).

2.8. Tissue preparation and immunofluorescence

Mice were euthanized by cervical dislocation. Brains were removed and fixed for 72 h with paraformaldehyde 4% (PFA), and then kept in PBS with 0.02% Sodium Azide at 4 °C until use. Coronal sections (40 μm) of the brain were obtained using a vibratome (Leica VT 1000S) and kept in cryoprotectant anti-freeze solution at −20 °C until use. Free-floating brain sections were rinsed twice in PBS for min and incubated 2 times for 15 min each with 50 mM NH_4Cl to reduce aldehyde-induced tissue autofluorescence. Sections were permeabilized twice for 10 min each with PBS containing 0.5% Triton X-100. Thereafter sections were blocked with PBS containing 0.3% Triton X-100, 0.2% sodium Azide and 5% normal donkey serum/goat serum (Pierce Biotechnology, Rockford, IL) for 2 h at room temperature. Then, sections were incubated overnight at 4 °C in the presence of primary antibodies in PBS-T: rabbit Foxp2 antibody (1:100, Abcam #ab16046, Cambrige, UK), mouse anti-DARPP-32 1:1000 (#611520, BD Transductions, San José, CA, USA). Sections were then washed three times and incubated for 2 h at room temperature with fluorescent secondary antibodies: Cy3 goat anti-rabbit (1:200) and/or AlexaFluor 488 donkey anti-mouse (1:200; both from Jackson ImmunoResearch, West Grove, PA, USA). No signal was detected in control sections incubated in the absence of the primary antibody.

2.9. Confocal imaging and analysis

Immunostained tissue sections (40-μm thick) containing striatum were imaged using a Leica Confocal SP5-II (20× or 40× numerical aperture lens, 5× digital zoom, 1-Airy unit pinhole). At least two slices per mouse, were analyzed, and up to two representative striatum images were obtained from each slice. Four frames were averaged per z-step throughout the study. Confocal z-stacks were taken at 1024 × 1024-pixel resolution every 2 μm. Foxp2 nuclei integrated optical density was quantified with NIH ImageJ freeware (Wayne Rasband, NIH).

2.10. Golgi Staining and dendritic spine analysis

Fresh brain hemispheres were processed following the Golgi-Cox method as described elsewhere(Giralt et al., 2017). Mouse brain hemispheres were incubated in the dark for 21 days in filtered dye solution consisted of 1% potassium dichromate, 1% mercury chloride and 0.8% potassium chromate. Consecutively brain tissue was washed 3 times for 2 min each in distilled water and 30 min in 90% ethanol. Thereafter, brain hemispheres were cut in 200 μm sections in 70% ethanol on a vibratome (Leica VT 1000S) and washed in distilled water for 5 min. The 200 μm sections were then reduced in 16% ammonia solution for 1 h, washed in water for 2 min and fixed in 1% sodium thiosulfate for 7 min. After reduction and a 2 min final wash in water, sections were mounted on super frost coverslips and dehydrated for 3 min in 50, 70, 80 and 100% ethanol, incubated twice for 5 min each in a 2:1 isopropanol/ethanol mixture, followed by 5 min incubation in pure isopropanol and twice incubation of 5 min each in xylol. Finally, samples were mounted with mounting medium (DPX, Merck) and let them dry. Secondary dendrites from striatum were photographed, with a maximum of two-three dendrites per neuron and from at least 3 slices per animal. *Z*-stacks from 0.2 μm sections were obtained in bright field at x63 resolution on a Widefield AF6000 Monochroma Camera Leica Microscope. Images were analyzed with the ImageJ software. Secondary dendritic segments (>20 μm long) were selected and traced. The total number of spines was obtained using the cell counter tool from ImageJ. Dendritic spine density was obtained after dividing the number of spines by the length of the segment (n° spines/μm). At least 60 dendrites per group from at least four mice per genotype were counted.

2.11. Immunoblot analysis

Animals were sacrificed by cervical dislocation. The brain was removed, and the striatum and cortex were rapidly dissected on ice and stored at −80 °C until use. Briefly, the tissue was lysed by sonication in ice-cold lysis buffer containing: 1% Triton X-100, 10% Glycerol, 50 mM Tris-HCl pH 7.5, 10 mM EDTA, 150 mM NaCl, supplemented with proteases and phosphatase inhibitors: 2 mM PMSF (from phenylmethylsulphonyl fluoride), 10 μg/ml Aprotinin,1 μg/ml Leupeptin, 2 mM Na3VO4 and 100 mM NaF and protease inhibitor cocktail (Sigma-Aldrich, St. Louis, MO, USA). Samples were centrifuged at 16,000*g* during 30 min at 4 °C. Supernatant proteins (15 μg) from total brain regions extracts were loaded in SDS–PAGE and transferred to nitrocellulose membranes (Whatman Schleicher & Schuell, Keene, NH, USA). Membranes were blocked in TBS-T (150 mM NaCl, 50 mM Tris-HCl, pH 7.4, 0.5 ml l^{-1} Tween 20) with 50 g l^{-1} non-fat dry milk and 50 g l^{-1} BSA. Membranes were immunoblotted at 4 °C with the following primary antibodies: Rabbit Foxp2 (1:1000, Abcam #ab16046, Cambrige, UK); mouse Ip6k2 (1:1000, Affinity Biosciences #DF8669); mouse Arhgap4 (1:1000, Santa Cruz #sc-376,251); rabbit Tor1A (1:1000, Proteintech #10296–1-AP) and rabbit Epb4.1/3 (1:1000, LifeSpan Biosciences #LS-C766264–60). After several washes in TBS-T, blots were incubated with secondary anti-rabbit (1:2000, Promega, Madison, Wi, USA). Membranes were developed using luminol reagent (Santa Cruz Biotechnology, Santa Cruz, CA, USA) in the Chemidoc MP Imaging System (Bio-Rad, California, USA). Gel-Pro densitometry program (Gel-Pro 3.2 Analyzer for Windows-version) was used to quantify the intensity of the different immunoreactive bands relative to the intensity of the loading controls. For loading control a mouse monoclonal antibody for a-tubulin was used.

2.12. Tissue processing for mass spectrometry assays

Lysates of 4-week-old mice striatum from Foxp2 overexpression experiment were processed for mass spectrometry (MaxQuant run, Proteomic facility, Max Planck Institute of Biochemistry, Martinsried, Germany) as previously described(del Toro et al., 2020).

2.13. Statistical analysis

Statistical analyses were carried out using the GraphPad Prism 8.0 software. Sample sizes were chosen using a power analysis: 0.05 alpha value, 1 estimated sigma value and 75%. No methods of randomization were used to allocate animals to experimental groups. Two-tailed

Student's *t*-test (95% confidence), one-way ANOVA or two-way ANOVA, with Tukey's *post hoc* multiple comparison test were performed as required. A p value <0.05 was considered significant.

3. Results

3.1. R6/1 mice at 4 weeks of age display impulsive-like behavior

We first aimed to explore in depth the earliest psychiatric-like phenotypes observable in the R6/1 mouse model. Thus, 4-week-old (juvenile) R6/1 mice and age-matched wild type (WT) controls were subjected to a set of behavioral tests (Fig. 1a). We measured exploratory activity in 15 min open-field test and we did not observe differences between genotypes in time in the center of the arena, suggesting similar levels of anxiety-like behavior in both groups (Fig. 1b). Furthermore, in the plus maze test both genotypes, R6/1 mice and WT littermates, spent similar percentage of the time in the open arms (Fig. 1c), confirming no differences in anxiety-like behavior between genotypes. We next assessed the presence of impulsive-like behavior by performing the cliff-avoidance jumping test. Interestingly, we observed that R6/1 mice manifest a significant increase in impulsive-like behavior by spending less time in the round platform than WT mice (Fig. 1d). Next, to test potential signs of depressive-like behavior we performed a forced swimming test, but we did not observe differences in immobility duration either, at the first 2 min (Fig. 1e) or at the last 4 min (Fig. 1f), suggesting no presence of depressive-like behaviors in 4-week-old R6/1 mice. In summary, 4-week-old R6/1 mice display impulsive-like symptoms.

3.2. Foxp2 protein levels are early decreased in the striatum of postnatal R6/1 mice

It has been shown that Foxp2 is reduced in mouse models of HD although those studies were focused in very advanced stages of the disease (Deng et al., 2021). Interestingly, Foxp2 alterations underlie several psychiatric-like behavioral deficits (Khanzada et al., 2017) including impulsivity, hyperactivity, and social disturbances (Medvedeva et al., 2019; Ribasés et al., 2012). Since we observed that juvenile R6/1 mice display similar psychiatric-like alterations we next analyzed Foxp2 protein levels in striatal and cortical extracts obtained from R6/1

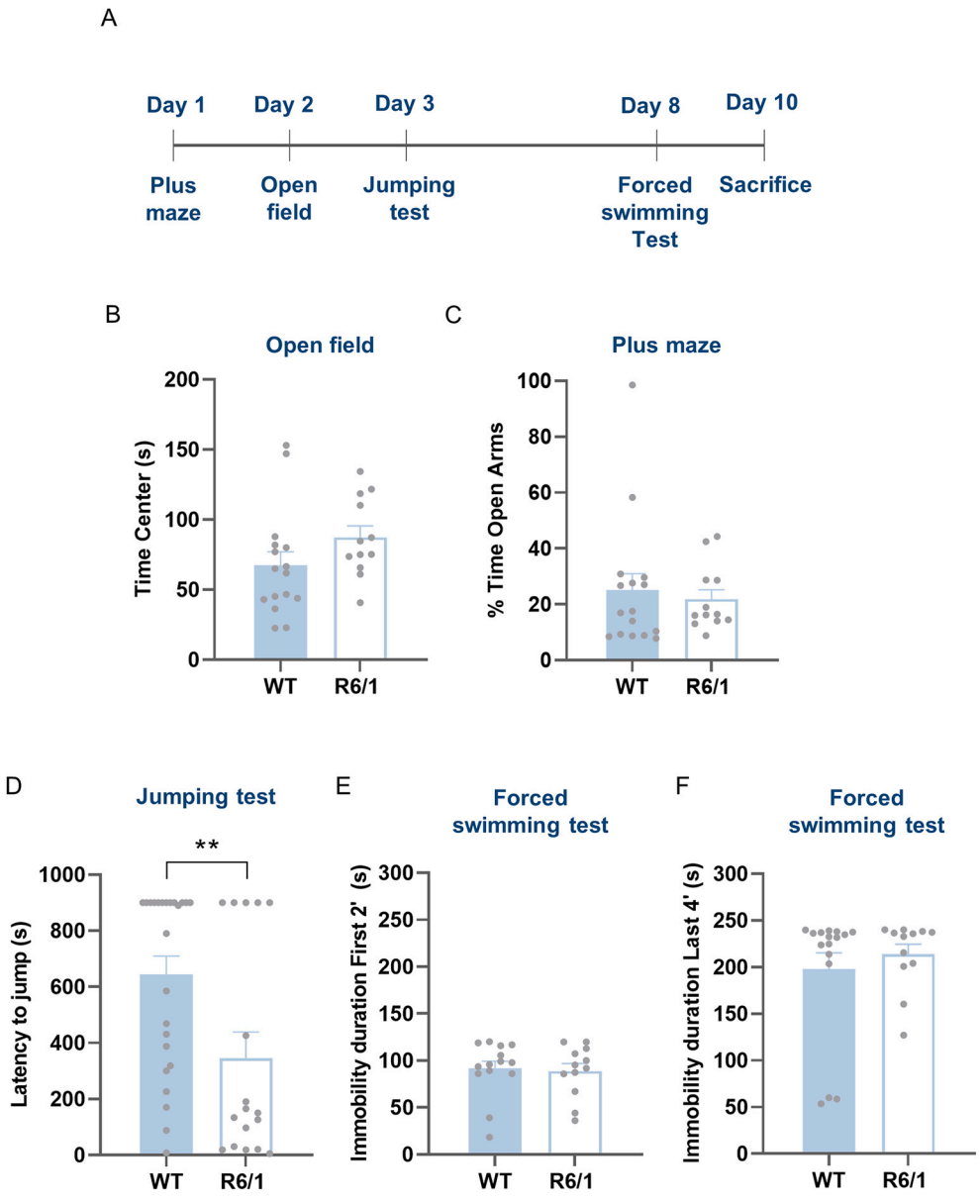

Fig. 1. Behavioral assessment of psychiatric-like disturbances in the 4-week-old R6/1 mice. (a) Timeline of behavioral testing in R6/1 mice and WT controls. (b) Time in the center of the open field apparatus during 15 min. (c) Time spent in the open arms of an elevated plus maze. (d) Latency to jump in the cliff avoidance test. Two-tailed Student's *t*-test: $t_{39} = 2.718$, $p = 0.0098$. (e) Forced swimming test: immobility duration during the first 2 min in a 6-min long session. (f) Forced swimming test: immobility duration during the last 4 min in a 6 min long session. Data are means + SEM. R6/1 ($n = 16$); WT ($n = 12$) for open field test, plus maze and forced swimming pole test. R6/1 ($n = 18$); WT ($n = 24$) for cliff avoidance test. ** $p <$ 0.01 compared to WT controls.

mice and WT controls. Striatal and cortical samples were analyzed along the disease progression and the different symptomatic stages: asymptomatic stage (PND3, PND15, 4 and 8 weeks), early symptomatic stage (12 weeks), and late symptomatic stage (20 weeks). Western blot analysis revealed that endogenous Foxp2 expression was significantly reduced from PND15, and remained downregulated at 4 weeks, 8 weeks, 12 weeks, and 20 weeks in the transgenic R6/1 mice striatal tissue compared to the age-matched WT mice (Fig. 2a-b). However, at the younger PND3, Foxp2 levels expression was similar between genotypes (Fig. 2a-b). Similarly, western blot analysis revealed that endogenous Foxp2 expression in cortical samples was reduced at 8 weeks, 12 weeks, and 20 weeks. However, at younger ages as PND3, PND15 or 4 weeks, Foxp2 expression was similar in the R6/1 mouse cortex compared to WT (Fig. 2c-d). To further investigate if the reduction of Foxp2 protein levels was restricted to different subregions or, in contrast, was homogenous in the whole striatum, we next performed an immunofluorescence against Foxp2 in the striatum of 4-week-old R6/1 mice and age-matched WT controls (Fig. 2e). Interestingly, we found a significant reduction of Foxp2 protein levels in the dorsal striatum R6/1 mice compared to WT littermates (Fig. 2f-g). However, in the Nucleus Accumbens the expression of Foxp2 protein was unchanged (Fig. 2h). To further expand our findings, we also evaluated striatal Foxp2 protein levels in the HdhQ7/Q111 heterozygous mice, a Knock in (KI) mouse model of Huntington's Disease. We found that at 6 months of age (Fig. 2i and k) as well as at 8 months of age (Fig. 2j-k) striatal Foxp2 protein levels were reduced in KI mice respect to WT mice. Interestingly, the onset of cognitive and motor phenotypes appear at those ages (Brito et al., 2014; Giralt et al., 2012; Puigdellívol et al., 2015). Altogether, we show for the first time a very early and persistent reduction of Foxp2 in R6/1 striatum that could potentially be involved with the development of the psychiatric-like symptoms observed in juvenile R6/1 mice.

3.3. Restoration of striatal Foxp2 levels improves the impulsivity-like phenotype in the 4-week-old R6/1 mice

We hypothesized that the early reduction of Foxp2 in the striatum could be involved in psychiatric-like symptoms observed in R6/1 mice. Thus, we next injected in the striatum of PND0-PND2 R6/1 mice and age-matched WT controls with an AAV to express Foxp2 under the control of CaMKII promoter, as a strategy to correct the downregulated striatal Foxp2 expression in R6/1 mice. R6/1 and WT mice control groups were injected with an AAV expressing only GFP. Both viruses were bilaterally injected in the striatum. Intriguingly, although the reduction of Foxp2 in the R6/1 striatum was homogeneous (Fig. 2e), the viral transduction displayed by the AAVs was predominantly a patchy-like distribution (Fig. 3a). Therefore we cannot rule out an effect of major over-expression of Foxp2 in patches than in matrix and that this could exert some effects in cognition as previously demonstrated by manipulating medium spiny neurons in each of these striatal sub-compartments (Friedman et al., 2020). Our results showed a clear recovery of Foxp2 levels in the striatal region of R6/1 mice injected with AAV expressing Foxp2 (Fig. 3a-c). Three weeks after surgery (in 4-week-old mice), all the groups, R6/1-GFP, R6/1-Foxp2, WT-GFP and WT-Foxp2 mice were subjected to a battery of striatum-dependent behavioral test (Fig. 3d). First, we assessed exploratory activity in a 15 min open-field test and found that the four experimental groups spent similar times in the center of the arena (Fig. 3e), suggesting that Foxp2 over-expression had not effects in anxiety-like behaviors. When the four experimental groups were subjected to the cliff avoidance jumping test, juvenile R6/1-GFP mice replicated previous impulsive-like behavior by spending less time in the round platform than WT-GFP. In contrast, R6/1-Foxp2 mice spent more time in the round platform than R6/1-GFP, reaching similar levels compared with WT-GFP group (Fig. 3f). Therefore, the correction of striatal Foxp2 levels in postnatal R6/1 pups restored their impulsivity-like behavior at 4-weeks of age. To further investigate the psychiatric-like alterations of the juvenile R6/1 mouse we performed a resident-intruder paradigm designed to assess aggressive-like behavior in mice. In this test, R6/1-GFP mice were less aggressive than WT-GFP. Concretely, less R6/1-GFP mice initiated a fight and the latency to start a fight also took longer compared to WT mice (Fig. 3g). Similarly, the duration of the fight of the R6/1 mice was shorter compared to WT mice (Fig. 3h), suggesting that 4-week-old R6/1 mice displayed less aggressive behavior than age-matched WT mice. Thus, the correction of striatal Foxp2 levels in R6/1 mice only partially corrected their social impairments (Fig. 3g). In summary, we show that early striatal Foxp2 downregulation is strongly associated to impulsivity-like behavior in R6/1 mice.

3.4. Restoration of striatal Foxp2 levels in 4-week-old R6/1 mice improves the altered expression of striatal proteins and rescues dendritic spine pathology

As some of the behavioral phenotypes showed by the juvenile R6/1 mice were improved by correcting striatal Foxp2 levels, we next focused on the identification of the potential underlying molecular mechanisms. We performed a protein expression screening in the striatum of transduced 4-week-old R6/1 mice and WT littermates from Fig. 3 using a mass spectrometry approach. As expected, and according to a very early and presymptomatic stage of the R6/1 mouse model, we found subtle changes in protein expression. A total of 35 proteins were differentially expressed between juvenile R6/1-GFP and WT-GFP mice. Thus, 19 of the aberrantly regulated proteins were downregulated whereas 16 proteins were upregulated (Fig. 4a-b). Most of the altered proteins (Epb4.1/3, Tbc1d19, Crocc.1, Dpysl4.1, Scarb2, Tor1a) were related with cytoskeleton dynamics such as vesicle trafficking (Downs et al., 2021; Lee et al., 2012), actin filament (Bahe et al., 2005; Castelnuovo et al., 2009; Nakamura et al., 2014) and GTPase activity (Ishibashi et al., 2009). Moreover, most of the aberrantly regulated candidate proteins observed in the R6/1 mice-GFP were restored with the correction of the striatal Foxp2 levels (Fig. 4c). Only 2 proteins remained altered Dpp6 and Arhgap4, whereas 6 new proteins such as Crip2, Fkbp1a, Fbxl18, Fth1 and Serinc3 were altered *de novo* by Foxp2 overexpression (Fig. 4b-c). These alterations in those 6 new proteins could be due to off-target or secondary effects of increasing Foxp2 in the ventral striatum where Foxp2 was not reduced (Fig. 2e and g). In other words, we did not rescue but over-expressed Foxp2 levels in R6/1-Foxp2 mice in a region (Nucleus Accumbens or NAcc) where it was not necessary. In this line, we cannot rule out a possible role of these unspecific proteomic changes in the R6/1-Foxp2 mice phenotypes.

Since many of the corrected striatal proteins detected by mass spectrometry observed in R6/1-Foxp2 mice were related with the cytoskeleton and actin dynamics we next analyzed the dendritic spine density in Golgi-impregnated striatal neurons in all four groups. The dendritic spine density in striatal neurons from R6/1-GFP mice was reduced compared to WT-GFP mice (Fig. 4d-e). In contrast, R6/1-Foxp2 mice displayed a significant greater density than R6/1-GFP reaching similar levels to those observed in WT-GFP mice (Fig. 4d-e), indicating that the correction of striatal Foxp2 levels in juvenile R6/1 mice completely rescued striatal spine density loss in the juvenile R6/1 mouse.

Finally, we aimed to validate some of the findings from the mass spectrometry experiment by assessing protein levels in western blot assays. We first analyzed Ip6k2 protein levels. As opposed in the mass spectrometry study, we did not confirm any change on protein levels for Ip6k2 in any group (Fig. 4f). In the same samples we also analyzed Arhgap4 (Fig. 4g). We observed an increase of Arhgap4 in R6/1-Foxp2 as occurred in the mass spectrometry experiment, but we did not detect changes in the R6/1-GFP mice. Finally, we assessed Tor1A protein levels (Fig. 4h) and we found a specific decrease in the R6/1-GFP compared with WT-GFP mice whereas Tor1A protein levels were rescued in R6/1-Foxp2 mice compared with their respective controls. In summary, we partially corroborated some of the results from mass

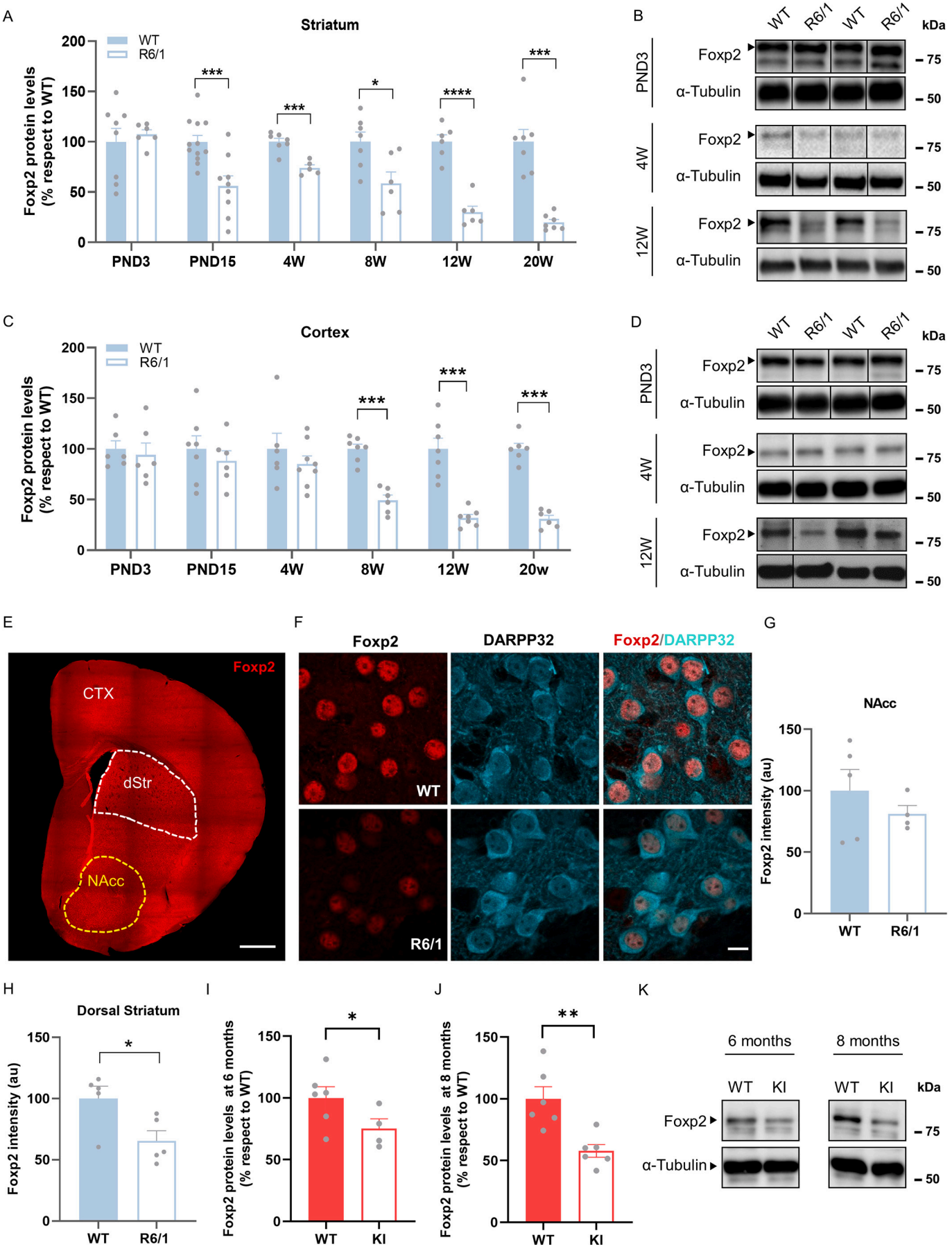

(caption on next page)

Fig. 2. Expression of endogenous Foxp2 in the R6/1 mouse striatum and cortex during the disease progression. (a) Densitometric quantification of striatal Foxp2 levels. Two-tailed Student's t-test: PND15 ($t_{19} = 3.896$, $p = 0.0010$), 4 weeks ($t_{10} = 4.325$, $p = 0.0003$), 8 weeks ($t_{11} = 2.808$, $p = 0.0170$), 12 weeks ($t_{10} = 7.775$, $p < 0.0001$) and 20 weeks ($t_{12} = 6.373$, $p < 0.0001$). Two-way ANOVA, time effect: ($F_{(5,74)} = 6.056$; $p < 0.0001$). (b) Immunoblotting analysis of Foxp2 and tubulin as a loading control. (c) Densitometric quantification of cortical Foxp2 levels. Two-tailed Student's t-test: 8 weeks ($t_{11} = 7.437$, $p < 0.0001$), 12 weeks ($t_{12} = 6.143$, $p < 0.0001$) and 20 weeks ($t_{10} = 10.70$, $p < 0.0001$). Two-way ANOVA, time effect: ($F_{(5,66)} = 5.271$; $p = 0.0004$). (d) Immunoblotting analysis of Foxp2 and tubulin as a loading control. (e) Photomicrograph showing Foxp2 expression in a WT brain mouse at 4 weeks of age. Scale bar, 500 μm. (f) Representative photomicrographs (high magnification) showing Foxp2 (red) nuclear expression and localization and DARPP32 (cyan) in the striatum of R6/1 mice and WT controls at 4 weeks of age. We analyzed 1 image per slice, 2 slices per mouse, 4–5 mice per group. Scale bar, 10 μm. (g) Quantification of the IOD average of Foxp2-positive nuclei in the NAcc as in e-f. (h) Quantification of the average of Foxp2-positive nuclei in the dorsal striatum as in e-f. Two-tailed Student's t-test: ($t_8 = 2.654$, $p = 0.0291$). (i) Densitometric quantification of striatal Foxp2 levels in Knock in (KI) mice at 6 months of age. Student's t-test ($t_8 = 1.924$, $p = 0.0453$). (j) Densitometric quantification of striatal Foxp2 levels in Knock in (KI) mice at 8 months of age. Student's t-test ($t_{10} = 3.824$, $p = 0.0017$). (k) Immunoblotting analysis of Foxp2 and tubulin as a loading control from i and j. Data are means + SEM. In a and c $n = 6$–12 mice / group, in g-h $n = 4$–5 mice / group, in i-j n = 4–6 mice / group. (For interpretation of the references to colour in this figure legend, the reader is referred to the web version of this article.)

spectrometry being the results from Tor1A the ones entirely validated.

3.5. Reduction of striatal Foxp2 in juvenile WT mice mimics the psychiatric-like phenotype observed in the juvenile R6/1 mice

We next aimed to verify whether a reduction of striatal Foxp2 is necessary and sufficient to provoke an increase of impulsivity-like behaviors and/or aggressive behaviors. To do so we bilaterally injected the striatum of PND0-PND2 WT mice with an AAV to express a shRNA against *Foxp2* as a strategy to mimic the striatal Foxp2 reduction observed in R6/1 mice observed in Fig. 2. As expected, we verified striatal Foxp2 reduction in the dorsal striatum (Fig. 5a-b) similar to that observed in juvenile R6/1 mice (Fig. 2). At 4 weeks of age, we subjected transduced WT mice with AAV-Scramble (WT-Scramble group) or with AAV-shFoxp2 (WT-sh-Foxp2 group) to the cliff-avoidance jumping test (Fig. 5c-d) and then to the resident-intruder test (Fig. 5c and e-f). We first observed that WT-sh-Foxp2 mice displayed shorter latencies to jump compared with WT-Scramble mice (Fig. 5d). Then, in the resident-intruder test we observed that WT-sh-Foxp2 mice showed increased latency to attack (Fig. 5e) and decreased fight duration (Fig. 5f) respect to WT-Scramble mice. In summary, Foxp2 reduction in the striatum at very young ages mimics the phenotypes observed in juvenile R6/1 mice.

4. Discussion

Here we have described a very early dysregulation of striatal Foxp2 protein levels which could be linked to early behavioral and molecular changes in the 4-week-old R6/1 mouse model. Interestingly, similar changes were replicated in the knock in (KI) mouse model of HD. At this age, R6/1 mice behavioral phenotype was characterized by increased impulsive-like behavior and less aggressive-like behavior concomitant with decreased dendritic spine density and dysregulation of striatal protein expression. Conversely, the overexpression of striatal Foxp2 levels in juvenile R6/1 mice reverted their impulsivity-phenotype, rescued the early striatal dendritic pathology and restored striatal protein dysregulation. Furthermore, inhibition of striatal Foxp2 expression in wild type mice mimicked the juvenile R6/1 early phenotypes described here.

Our findings highly recapitulate the pre-symptomatic HD clinical scenario, in which the appearance of the main psychiatric alterations occurs long before the first motor abnormalities, which have been classically related to a fronto-striatal dysfunction (Epping et al., 2016; Goh et al., 2018; Thompson et al., 2012). Regarding to the aggressive dimension it has been shown that HD knock in mice as well as R6/2 mice have a lack of interest for the intruder at late stages of the disease compared to WT mice (Shelbourne et al., 1999; Wood and Morton, 2015). Our study indicates that this phenotype is observable as early as at 4 weeks of age, an indicator that these alterations have a very earlier onset than motor symptoms. Finally, although we found changes on impulsivity and sociability in young R6/1 mice, in other dimensions such as depression-like behaviors we found no differences. The latter result must be taken with caution since we performed only one test and depressive-like symptoms are also detected very early in HD mouse models (Brito et al., 2019; Pla et al., 2014). Further studies should be performed in the future to fully address the role of Foxp2 in early depressive-like symptoms in HD mouse models.

Concurrent with the psychiatric-like phenotypes, we identified an early downregulation of Foxp2 striatal levels in the R6/1 mice since postnatal day 15, which was consistently maintained in the consecutives 4, 8, 12 and 20-week-old R6/1 mice. Although not so early in time, Foxp2 levels were also reduced in the cortex of the R6/1 mice. Consistently, the aforementioned brain regions could constitute a well-known neural substrates underlying the observed behavioral deficits (Dalley and Robbins, 2017; Lischinsky and Lin, 2020). Altogether these results suggest that early psychiatric-like manifestations in the R6/1 mice occur when Foxp2 is specifically reduced in the dorsal striatum.

As previously mentioned, the *Foxp2* gene is considered a potential susceptibility locus for many neuropsychiatric disorders (Khanzada et al., 2017). In the Foxp2 rescue experiments, only impulsivity levels of juvenile R6/1 mice were entirely restored reaching similar levels compared to WT mice. Disadvantageously, the relationship between Foxp2 and impulsivity has been poorly addressed in animal studies, on the contrary GWAS analyses in humans have extensively established the implication of *FOXP2* locus with Attention-Deficit Hyperactivity Disorder (ADHD), and the associated *impulsivity* dimension (Demontis et al., 2019). Interestingly, a mouse model with reduced Foxp2 levels showed increased impulsive-like behavior concomitant with molecular changes in the dorsal striatum (Jhang et al., 2017). Altogether, we conclude that the impulsive phenotype in juvenile R6/1 mice could be due to the Foxp2 dysregulation in the dorsal striatum *per se*. Also, a partial recovery of the aggressive-like behavior was observed in R6/1-Foxp2 mice, suggesting that striatal Foxp2 could modulate these alterations. Our mimicking experiments reinforced such idea. Supporting the role of striatal Foxp2 in the regulation of aggressive-behaviors in HD, in a previous study, *Foxp2* heterozygous mice revealed significant deficits in male territorial aggression by displaying smaller number of attacks, and shorter durations of the fights in a resident-intruder task (Herrero et al., 2021).

Regarding histopathological changes, we described for the first time a reduction of the spine density in the striatum as soon as in 4-week-old R6/1 mice as described elsewhere for much more advanced stages (Spires et al., 2004). The rescue of Foxp2 levels successfully rescued the dendritic spine loss in the striatum of R6/1 mice. These data are consistent with previous findings in the literature suggesting Foxp2 as a positive regulator of spines in several regions and animal models (Chen et al., 2016; Enard et al., 2009), and places this neuropathological event as one of the earliest in the progression of the disease. In contrast, we did not observe changes on spine density when over-expressing Foxp2 in wild type striatal neurons as previously reported in over-expressing Foxp2 cortical neurons (Sia et al., 2013). This discrepancy could be due to different regional properties (striatum *vs* cortex), system used (*in vivo* mice *vs* cultured cortical neurons) and methodology employed (transduction *vs* transfection).

Noteworthy, in our mass spectrometry study, a total of 35 proteins

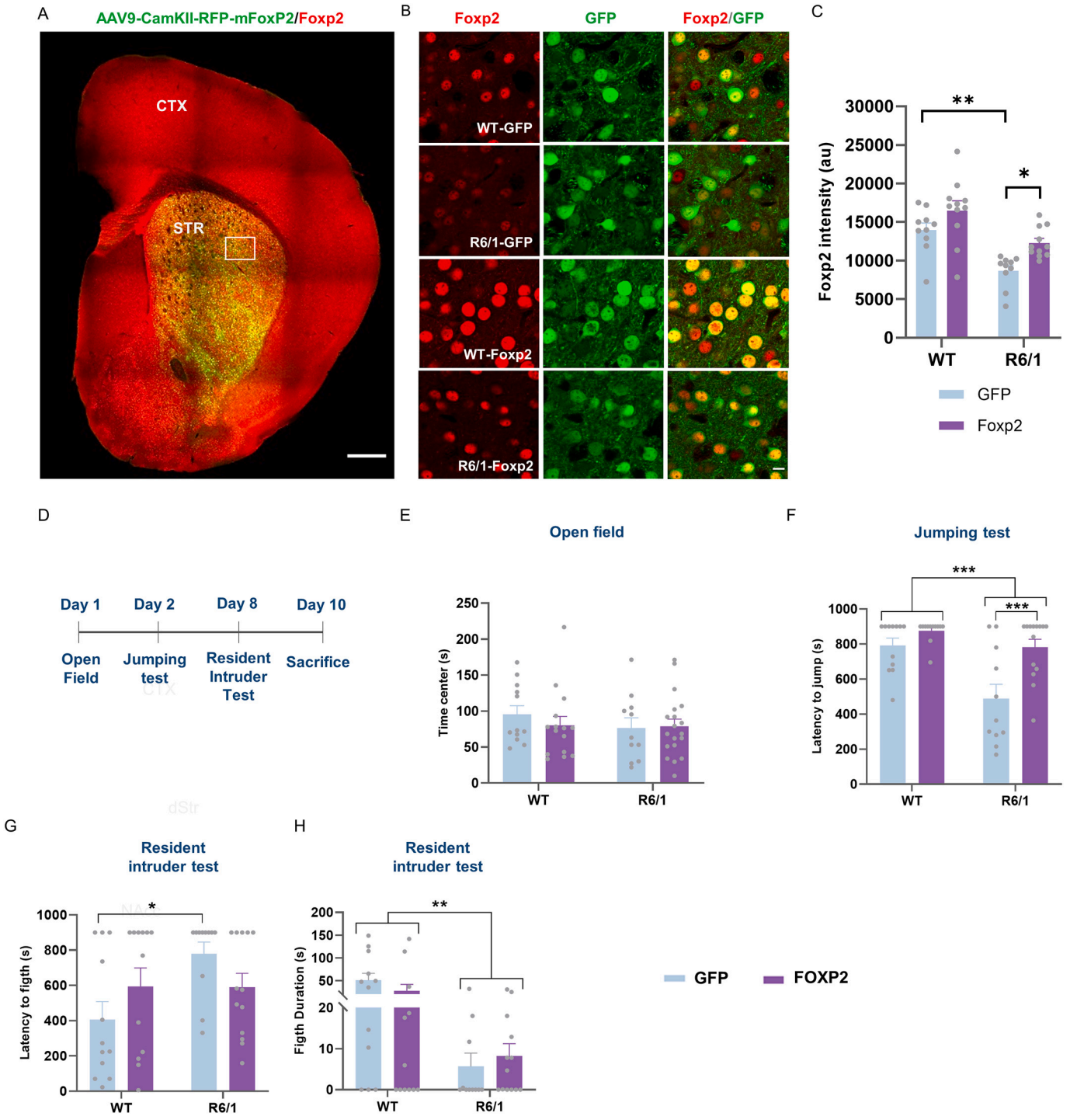

Fig. 3. Behavioral assessment of psychiatric-like disturbances in the 4-week-old R6/1-Foxp2 mice. (a) Expression and distribution of Foxp2 (in red) in the transduced (in green) juvenile R6/1 mice. Scale bar, 500 μm. (b) Representative photomicrographs (High magnification of inset in a) showing Foxp2 (red) nuclear expression and localization in R6/1-GFP, WT-GFP, R6/1-Foxp2 and WT-Foxp2 mice. Scale bar, 10 μm. (c) Quantification of the integrated optical density (IOD, arbitrary units) of the transduced Foxp2-positive nuclei in the striatum as in b. Two-way ANOVA, group effect: $F_{(1,38)} = 26.79$; $p < 0.0001$; treatment effect: $F_{(1,38)} = 11.19$; $p = 0.0019$. R6/1 GFP ($n = 10$); WT GFP (n = 10), R6/1 Foxp2 (n = 12); WT Foxp2 ($n = 11$). Tukey's *post hoc* test was used * $p < 0.05$ and ** $p < 0.01$ compared to WT controls. (d) Timeline of behavioral testing in the transduced juvenile R6/1 mice and WT controls. (e) Time in the center of the open field apparatus during 15 min. (f) Latency to jump in the cliff avoidance test. Two-way ANOVA, group effect: $F_{(1,45)} = 15.26$; $p = 0.0003$; treatment effect: $F_{(1,45)} = 13.78$; $p = 0.0006$; interaction effect: $F_{(1,45)} = 4.192$; $p = 0.0465$. (g) Latency to fight in the resident intruder test. Two-way ANOVA, group effect: $F_{(1,44)} = 4.252$; $p = 0.0451$; interaction effect: $F_{(1,44)} = 4.368$; $p = 0.0424$ (h) Duration of the fight in the resident intruder test. Two-way ANOVA, group effect: $F_{(1,44)} = 9.459$; $p = 0.0036$. Data are means + SEM. WT-GFP (n = 12), R6/1 GFP (n = 11); WT Foxp2 (n = 12); R6/1 Foxp2 ($n = 14$). Tukey's *post hoc* test was used in all experiments. (For interpretation of the references to colour in this figure legend, the reader is referred to the web version of this article.)

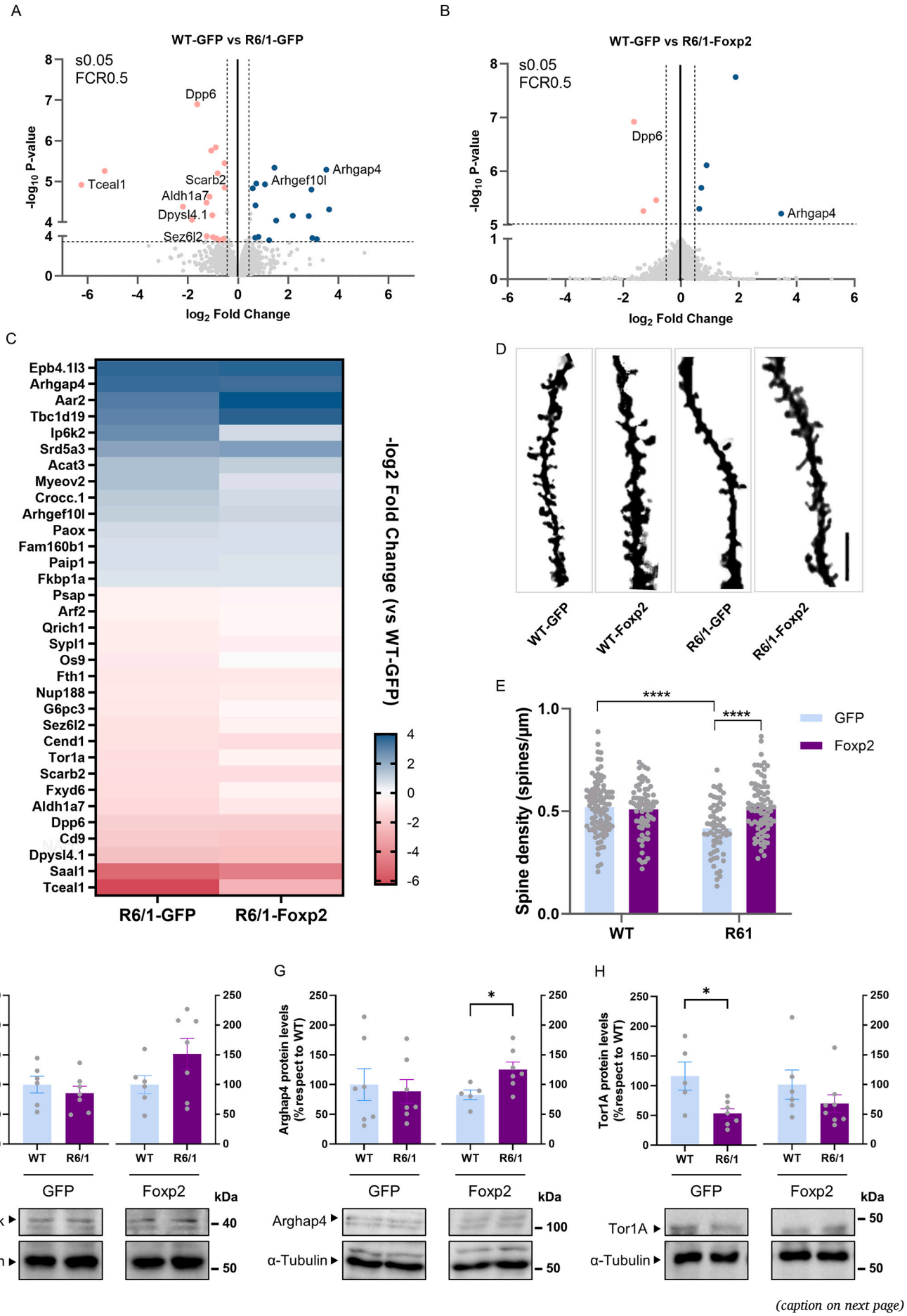

(caption on next page)

Fig. 4. Molecular and microstructural analysis of the 4-week-old R6/1-Foxp2 mice striatum. (a) Volcano plot of downregulated (red) and upregulated proteins (blue) of R6/1-GFP striatum respect to WT-GFP mice. (b) Volcano plot of downregulated (red) and upregulated proteins (blue) of R6/1-Foxp2 mice striatum respect to WT-GFP mice. (c) Heat map of clusters of downregulated (red) and upregulated proteins (blue) of R6/1-GFP and R6/1-Foxp2 mice striatum respect to WT-GFP mice. Cutoffs of ±0.5-fold change and $p < 0.05$. (n = 4 mice / group). (d) Golgi-Cox-stained dendrites from medium spiny neurons in the dorsal striatum. Scale bar, 7 μm. (e) Quantification of spine density in dendrites as in d. Two-way ANOVA, group effect: $F_{(1,302)} = 9.678$; $p = 0.0020$; treatment effect: $F_{(1,302)} = 9.728$; p = 0.0020; interaction effect: $F_{(1,302)} = 14.65$; $p = 0.0002$. Sidak's *post hoc* test (15 dendrites per animal / 4–5 mice / group). Densitometric quantification of striatal Ip6k2 (f), Arhgap4 (g) and Tor1A (h) protein levels in WT-GFP, R6/1-GFP, WT-Foxp2 and R6/1-Foxp2 mice. As a loading control α-tubulin was used in f-h. Data are means ± SEM. WT-GFP ($n = 7$), R6/1 GFP (n = 7); WT Foxp2 (n = 7); R6/1 Foxp2 (n = 7). (For interpretation of the references to colour in this figure legend, the reader is referred to the web version of this article.)

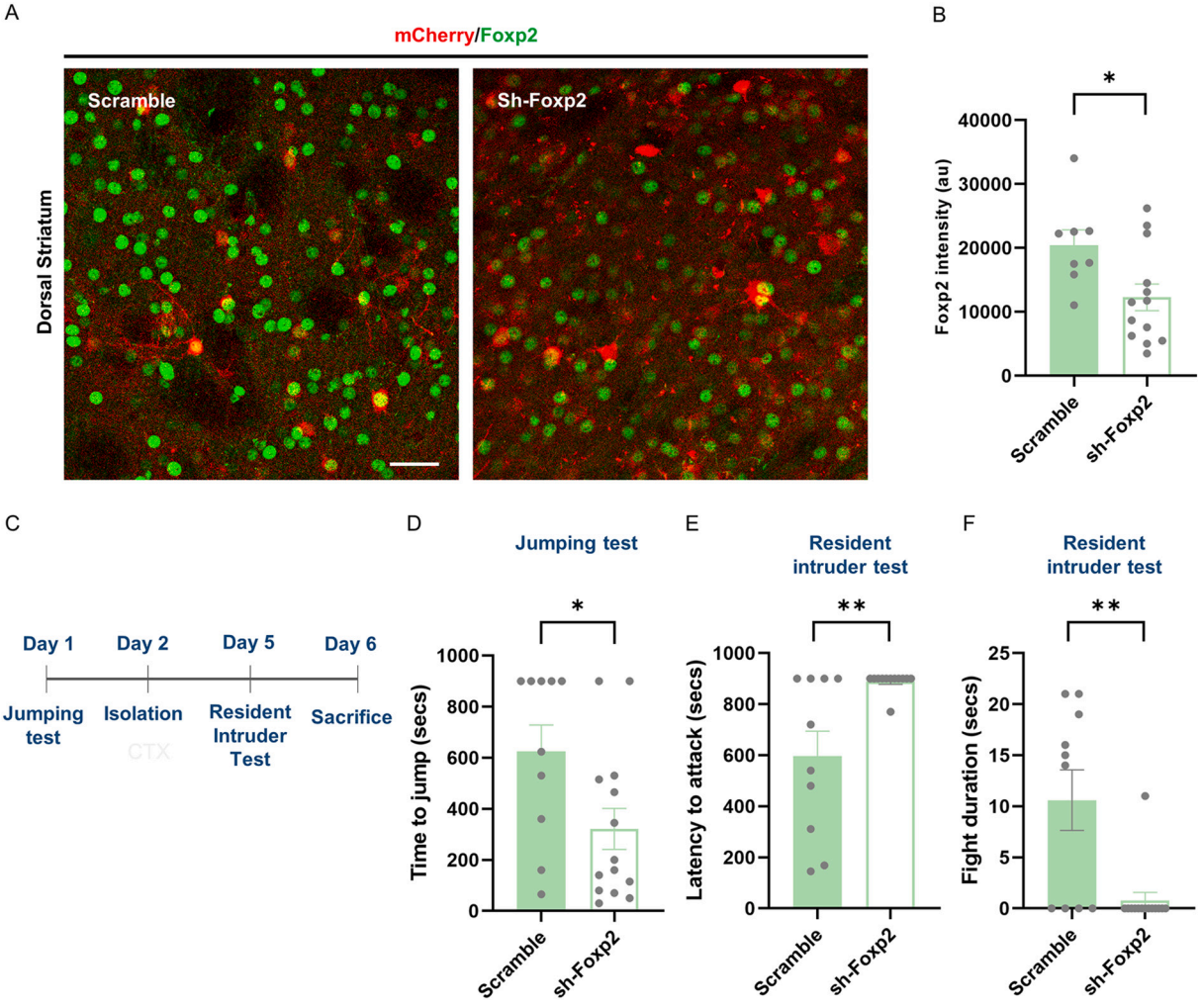

Fig. 5. Behavioral characterization and validation of 4-week-old wild type mice transduced with AAV-shRNA-Foxp2. (a) Expression and distribution of Foxp2 (in green) in the transduced juvenile wild type (WT) mice with scramble (red, left panel) or sh-RNA-Foxp2 (red, right panel). Scale bar, 40 μm. (b) Quantification of the integrated optical density (IOD, arbitrary units) of the transduced Foxp2-positive nuclei in the striatum as in a. Student t-test (Two-tailed Student's t-test: $t_{19} = 2.514$, $p = 0.0211$). (c) Timeline of the behavioral testing in the 4-week-old WT-Scramble and WT-sh-Foxp2 mice. (d) Latency to jump in the cliff avoidance test. Student t-test (Two-tailed Student's t-test: $t_{22} = 2.333$, $p = 0.0292$). (e) Latency to fight in the resident-intruder test. Student t-test (Two-tailed Student's t-test: $t_{22} = 3.251$, $p = 0.0040$). (f) Duration of the fight in the resident-intruder test. Student t-test Two-tailed Student's t-test: $t_{22} = 3.688$, $p = 0.0013$). WT-Scramble (n = 10); WT-sh-Foxp2 (n = 14). Data are means ± SEM. (For interpretation of the references to colour in this figure legend, the reader is referred to the web version of this article.)

were differentially expressed between juvenile R6/1-GFP and WT-GFP. Specifically, 19 of the aberrantly regulated candidate proteins were downregulated such as Tceal1, Tor1A and Scarb2 and 16 were upregulated such as Arhgef10l and Arhgap4. Most of the altered proteins are related with cytoskeleton dynamics as vesicle trafficking, actin filament and GTPase activity (Bahe et al., 2005; Castelnuovo et al., 2009; Downs et al., 2021; Ishibashi et al., 2009; Lee et al., 2012; Nakamura et al., 2014). From these results, we estimated that the early decrease in spine density might be associated with the dysregulation of several of these proteins, particularly Tor1A (Maltese et al., 2018), given that all the synaptic processes mentioned before are a keystone in the formation and stabilization of spine (Penzes and Cahill, 2012).

Furthermore, we found changes in several proteins related with psychiatric disorders. Arhgap4, Sez6l2, Tceal1 and Dpsyl4 are associated with schizophrenia (Ambalavanan et al., 2016; Bilecki et al., 2021; Wong et al., 2014), Aldh1a and Scarb2 are associated with risk-taking behavior (Lewohl et al., 2011; Lind et al., 2008), while Arhgef10l is related to insomnia (Lane et al., 2017). Interestingly, most of the aberrantly regulated candidate proteins were restored by rescuing Foxp2 levels, although only 2 candidate proteins remained altered namely

Dpp6 and Arhgap4. Furthermore, changes in the expression of 6 new proteins such as Crip2, Fkbp1a, Fbxl18, Fth1 and Serinc3 appeared as a secondary effect of Foxp2 overexpression. This myriad of affected proteins in R6/1-GFP that were in turn recovered in R6/1-Foxp2 mice support the role of Foxp2 in their direct or indirect regulation and suggest that such alterations might underly the neuropsychiatric-like phenotypes observed in the juvenile R6/1 mice. However, since we validated only some of the detected changes (Tor1A and partially Arhgap4) our conclusions from the mass spectrometry study must be taken with caution.

In summary, we identified an unanticipated new role of Foxp2 in the regulation of some of the earliest neuropsychiatric-like phenotypes in a HD mouse model which are among the most detrimental for the patients' welfare (Ho et al., 2009). Also, these findings could have relevant implications for the design of novel and future therapeutic strategies to counteract these specific and early symptoms.

CRediT authorship contribution statement

Ened Rodríguez-Urgellés: Conceptualization, Methodology, Investigation, Writing – original draft. **Irene Rodríguez-Navarro:** Validation, Formal analysis, Investigation. **Iván Ballasch:** Formal analysis, Investigation. **Daniel del Toro:** Resources, Conceptualization. **Verónica Brito:** Resources, Conceptualization. **Jordi Alberch:** Resources, Funding acquisition, Writing – review & editing. **Albert Giralt:** Conceptualization, Funding acquisition, Writing – original draft, Writing – review & editing.

Declaration of Competing Interest

The authors declare no conflict of interest.

Data availability

Data will be made available on request.

Acknowledgements

AG and DdT are Ramón y Cajal fellows (RYC-2016-19466 and RYC-2017-23486 respectively). This work was also supported by grants from Ministerio de Ciencia e Innovación/ AEI/https://doi.org/10.13039/501100011033/ and "FEDER": JA: PID2020-119386RB-100, AG: PID2021-122258OB-I00 and DdT: PID2021-124852OB-100. We thank Ana López (María de Maeztu Unit of Excellence, Institute of Neurosciences, University of Barcelona, MDM-2017-0729, Ministerio de Ciencia e Innovación) and Maite Muñoz (University of Barcelona) for technical support. We thank María Calvo from the Advanced Microscopy Service (Centres Científics i Tecnològics Universitat de Barcelona) for her help in the acquisition, analysis, and interpretation of the confocal images.

References

Ambalavanan, A., Girard, S.L., Ahn, K., Zhou, S., Dionne-Laporte, A., Spiegelman, D., Bourassa, C.V., Gauthier, J., Hamdan, F.F., Xiong, L., Dion, P.A., Joober, R., Rapoport, J., Rouleau, G.A., 2016. De novo variants in sporadic cases of childhood onset schizophrenia. Eur. J. Hum. Genet. 24, 944–948. https://doi.org/10.1038/ejhg.2015.218.

Bahe, S., Stierhof, Y.-D., Wilkinson, C.J., Leiss, F., Nigg, E.A., 2005. Rootletin forms centriole-associated filaments and functions in centrosome cohesion. J. Cell Biol. 171, 27–33. https://doi.org/10.1083/jcb.200504107.

Bilecki, W., Wawrzczak-Bargieła, A., Majcher-Maślanka, I., Chmelova, M., Maćkowiak, M., 2021. Inhibition of BET proteins during adolescence affects prefrontal cortical development: relevance to schizophrenia. Int. J. Mol. Sci. 22, 8710. https://doi.org/10.3390/ijms22168710.

Brito, V., Giralt, A., Enriquez-Barreto, L., Puigdellívol, M., Suelves, N., Zamora-Moratalla, A., Ballesteros, J.J., Martín, E.D., Dominguez-Iturza, N., Morales, M., Alberch, J., Ginés, S., 2014. Neurotrophin receptor p75NTR mediates Huntington's disease–associated synaptic and memory dysfunction. J. Clin. Invest. 124, 4411–4428. https://doi.org/10.1172/JCI74809.

Brito, V., Giralt, A., Masana, M., Royes, A., Espina, M., Sieiro, E., Alberch, J., Castañé, A., Girault, J.-A., Ginés, S., 2019. Cyclin-dependent kinase 5 dysfunction contributes to depressive-like behaviors in Huntington's disease by altering the DARPP-32 phosphorylation status in the nucleus Accumbens. Biol. Psychiatry 86, 196–207. https://doi.org/10.1016/j.biopsych.2019.03.001.

Castelnuovo, M., Monticone, M., Massone, S., Vassallo, I., Tortelli, F., Cancedda, R., Pagano, A., 2009. Rolly protein (ROLP)-Epb4.1/3: a potential protein-protein interaction relevant for the maintenance of cell adhesion. Int. J. Mol. Sci. 10, 2054–2065. https://doi.org/10.3390/ijms10052054.

Cepeda, C., Wu, N., Andre, V., Cummings, D., Levine, M., 2007. The corticostriatal pathway in Huntington's disease. Prog. Neurobiol. 81, 253–271. https://doi.org/10.1016/j.pneurobio.2006.11.001.

Chen, Y.-C., Kuo, H.-Y., Bornschein, U., Takahashi, H., Chen, S.-Y., Lu, K.-M., Yang, H.-Y., Chen, G.-M., Lin, J.-R., Lee, Y.-H., Chou, Y.-C., Cheng, S.-J., Chien, C.-T., Enard, W., Hevers, W., Pääbo, S., Graybiel, A.M., Liu, F.-C., 2016. Foxp2 controls synaptic wiring of corticostriatal circuits and vocal communication by opposing Mef2c. Nat. Neurosci. 19, 1513–1522. https://doi.org/10.1038/nn.4380.

Chiu, C.-T., Liu, G., Leeds, P., Chuang, D.-M., 2011. Combined treatment with the mood stabilizers Lithium and valproate produces multiple beneficial effects in transgenic mouse models of Huntington's disease. Neuropsychopharmacology 36, 2406–2421. https://doi.org/10.1038/npp.2011.128.

Dalley, J.W., Robbins, T.W., 2017. Fractionating impulsivity: neuropsychiatric implications. Nat. Rev. Neurosci. 18, 158–171. https://doi.org/10.1038/nrn.2017.8.

del Toro, D., Carrasquero-Ordaz, M.A., Chu, A., Ruff, T., Shahin, M., Jackson, V.A., Chavent, M., Berbeira-Santana, M., Seyit-Bremer, G., Brignani, S., Kaufmann, R., Lowe, E., Klein, R., Seiradake, E., 2020. Structural basis of Teneurin-Latrophilin interaction in repulsive guidance of migrating neurons. Cell 180, 323–339.e19. https://doi.org/10.1016/j.cell.2019.12.014.

Demontis, D., Walters, R.K., Martin, J., Mattheisen, M., Als, T.D., Agerbo, E., Baldursson, G., Belliveau, R., Bybjerg-Grauholm, J., Bækvad-Hansen, M., Cerrato, F., Chambert, K., Churchhouse, C., Dumont, A., Eriksson, N., Gandal, M., Goldstein, J.I., Grasby, K.L., Grove, J., Gudmundsson, O.O., Hansen, C.S., Hauberg, M.E., Hollegaard, M.V., Howrigan, D.P., Huang, H., Maller, J.B., Martin, A.R., Martin, N. G., Moran, J., Pallesen, J., Palmer, D.S., Pedersen, C.B., Pedersen, M.G., Poterba, T., Poulsen, J.B., Ripke, S., Robinson, E.B., Satterstrom, F.K., Stefansson, H., Stevens, C., Turley, P., Walters, G.B., Won, H., Wright, M.J., Andreassen, O.A., Asherson, P., Burton, C.L., Boomsma, D.I., Cormand, B., Dalsgaard, S., Franke, B., Gelernter, J., Geschwind, D., Hakonarson, H., Haavik, J., Kranzler, H.R., Kuntsi, J., Langley, K., Lesch, K.-P., Middeldorp, C., Reif, A., Rohde, L.A., Roussos, P., Schachar, R., Sklar, P., Sonuga-Barke, E.J.S., Sullivan, P.F., Thapar, A., Tung, J.Y., Waldman, I.D., Medland, S.E., Stefansson, K., Nordentoft, M., Hougaard, D.M., Werge, T., Mors, O., Mortensen, P.B., Daly, M.J., Faraone, S.V., Børglum, A.D., Neale, B.M., 2019. Discovery of the first genome-wide significant risk loci for attention deficit/hyperactivity disorder. Nat. Genet. 51, 63–75. https://doi.org/10.1038/s41588-018-0269-7.

Deng, Y., Wang, H., Joni, M., Sekhri, R., Reiner, A., 2021. Progression of basal ganglia pathology in heterozygous <scp>Q175</scp> knock-in Huntington's disease mice. J. Comp. Neurol. 529, 1327–1371. https://doi.org/10.1002/cne.25023.

Dorsey, R., Biglan, K., Eberly, S., Auinger, P., Brocht, A., Umeh, C.C., Oakes, D., Clarence-Smith, K., Marshall, F., Shoulson, I., Frank, S., 2011. Use of Tetrabenazine in Huntington disease patients on antidepressants or with advanced disease: results from the TETRA-HD study. PLoS Curr. 3, RRN1283. https://doi.org/10.1371/currents.RRN1283.

Downs, A.M., Fan, X., Kadakia, R.F., Donsante, Y., Jinnah, H.A., Hess, E.J., 2021. Cell-intrinsic effects of TorsinA(ΔE) disrupt dopamine release in a mouse model of TOR1A dystonia. Neurobiol. Dis. 155, 105369 https://doi.org/10.1016/j.nbd.2021.105369.

Enard, W., Gehre, S., Hammerschmidt, K., Hölter, S.M., Blass, T., Somel, M., Brückner, M. K., Schreiweis, C., Winter, C., Sohr, R., Becker, L., Wiebe, V., Nickel, B., Giger, T., Müller, U., Groszer, M., Adler, T., Aguilar, A., Bolle, I., Calzada-Wack, J., Dalke, C., Ehrhardt, N., Favor, J., Fuchs, H., Gailus-Durner, V., Hans, W., Hölzlwimmer, G., Javaheri, A., Kalaydjiev, S., Kallnik, M., Kling, E., Kunder, S., Moßbrugger, I., Naton, B., Racz, I., Rathkolb, B., Rozman, J., Schrewe, A., Busch, D.H., Graw, J., Ivandic, B., Klingenspor, M., Klopstock, T., Ollert, M., Quintanilla-Martinez, L., Schulz, H., Wolf, E., Wurst, W., Zimmer, A., Fisher, S.E., Morgenstern, R., Arendt, T., Hrabé de Angelis, M., Fischer, J., Schwarz, J., Pääbo, S., 2009. A humanized version of Foxp2 affects Cortico-basal ganglia circuits in mice. Cell 137, 961–971. https://doi.org/10.1016/j.cell.2009.03.041.

Epping, E.A., Kim, J.-I., Craufurd, D., Brashers-Krug, T.M., Anderson, K.E., McCusker, E., Luther, J., Long, J.D., Paulsen, J.S., 2016. Longitudinal psychiatric symptoms in prodromal Huntington's disease: a decade of data. Am. J. Psychiatry 173, 184–192. https://doi.org/10.1176/appi.ajp.2015.14121551.

Friedman, A., Hueske, E., Drammis, S.M., Toro Arana, S.E., Nelson, E.D., Carter, C.W., Delcasso, S., Rodriguez, R.X., Lutwak, H., DiMarco, K.S., Zhang, Q., Rakocevic, L.I., Hu, D., Xiong, J.K., Zhao, J., Gibb, L.G., Yoshida, T., Siciliano, C.A., Diefenbach, T.J., Ramakrishnan, C., Deisseroth, K., Graybiel, A.M., 2020. Striosomes mediate value-based learning vulnerable in age and a Huntington's disease model. Cell 183, 918–934.e49. https://doi.org/10.1016/j.cell.2020.09.060.

Giralt, A., Puigdellivol, M., Carreton, O., Paoletti, P., Valero, J., Parra-Damas, A., Saura, C.A., Alberch, J., Gines, S., 2012. Long-term memory deficits in Huntington's disease are associated with reduced CBP histone acetylase activity. Hum. Mol. Genet. 21, 1203–1216. https://doi.org/10.1093/hmg/ddr552.

Giralt, A., Brito, V., Chevy, Q., Simonnet, C., Otsu, Y., Cifuentes-Díaz, C., de Pins, B., Coura, R., Alberch, J., Ginés, S., Poncer, J.-C., Girault, J.-A., 2017. Pyk2 modulates hippocampal excitatory synapses and contributes to cognitive deficits in a

Huntington's disease model. Nat. Commun. 8, 15592. https://doi.org/10.1038/ncomms15592.
Goh, A.M., Wibawa, P., Loi, S.M., Walterfang, M., Velakoulis, D., Looi, J.C., 2018. Huntington's disease: neuropsychiatric manifestations of Huntington's disease. Australas. Psychiatry 26, 366–375. https://doi.org/10.1177/1039856218791036.
Gusella, J.F., Wexler, N.S., Conneally, P.M., Naylor, S.L., Anderson, M.A., Tanzi, R.E., Watkins, P.C., Ottina, K., Wallace, M.R., Sakaguchi, A.Y., Young, A.B., Shoulson, I., Bonilla, E., Martin, J.B., 1983. A polymorphic DNA marker genetically linked to Huntington's disease. Nature 306, 234–238. https://doi.org/10.1038/306234a0.
Hachigian, L.J., Carmona, V., Fenster, R.J., Kulicke, R., Heilbut, A., Sittler, A., Pereira de Almeida, L., Mesirov, J.P., Gao, F., Kolaczyk, E.D., Heiman, M., 2017. Control of Huntington's disease-associated phenotypes by the striatum-enriched transcription factor Foxp2. Cell Rep. 21, 2688–2695. https://doi.org/10.1016/j.celrep.2017.11.018.
Häring, M., Enk, V., Aparisi Rey, A., Loch, S., Ruiz de Azua, I., Weber, T., Bartsch, D., Monory, K., Lutz, B., 2015. Cannabinoid type-1 receptor signaling in central serotonergic neurons regulates anxiety-like behavior and sociability. Front. Behav. Neurosci. 9 https://doi.org/10.3389/fnbeh.2015.00235.
Herrero, M.J., Wang, L., Hernandez-Pineda, D., Banerjee, P., Matos, H.Y., Goodrich, M., Panigrahi, A., Smith, N.A., Corbin, J.G., 2021. Sex-specific social behavior and amygdala proteomic deficits in Foxp2+/− mutant mice. Front. Behav. Neurosci. 15 https://doi.org/10.3389/fnbeh.2021.706079.
Ho, A.K., Gilbert, A.S., Mason, S.L., Goodman, A.O., Barker, R.A., 2009. Health-related quality of life in Huntington's disease: which factors matter most? Mov. Disord. 24, 574–578. https://doi.org/10.1002/mds.22412.
Ishibashi, K., Kanno, E., Itoh, T., Fukuda, M., 2009. Identification and characterization of a novel Tre-2/Bub2/Cdc16 (TBC) protein that possesses Rab3A-GAP activity. Genes Cells 14, 41–52. https://doi.org/10.1111/j.1365-2443.2008.01251.x.
Jhang, C.-L., Huang, T.-N., Hsueh, Y.-P., Liao, W., 2017. Mice lacking cyclin-dependent kinase-like 5 manifest autistic and ADHD-like behaviors. Hum. Mol. Genet. 26, 3922–3934. https://doi.org/10.1093/hmg/ddx279.
Khanzada, N., Butler, M., Manzardo, A., 2017. GeneAnalytics pathway analysis and genetic overlap among autism Spectrum disorder, bipolar disorder and schizophrenia. Int. J. Mol. Sci. 18, 527. https://doi.org/10.3390/ijms18030527.
Lane, J.M., Liang, J., Vlasac, I., Anderson, S.G., Bechtold, D.A., Bowden, J., Emsley, R., Gill, S., Little, M.A., Luik, A.I., Loudon, A., Scheer, F.A.J.L., Purcell, S.M., Kyle, S.D., Lawlor, D.A., Zhu, X., Redline, S., Ray, D.W., Rutter, M.K., Saxena, R., 2017. Genome-wide association analyses of sleep disturbance traits identify new loci and highlight shared genetics with neuropsychiatric and metabolic traits. Nat. Genet. 49, 274–281. https://doi.org/10.1038/ng.3749.
Lee, D., Desmond, M.J., Fraser, S.A., Katerelos, M., Gleich, K., Berkovic, S.F., Power, D. A., 2012. Expression of the transmembrane lysosomal protein SCARB2/Limp-2 in renin secretory granules controls renin release. Nephron Exp. Nephrol. 122, 103–113. https://doi.org/10.1159/000350737.
Lewohl, J.M., Nunez, Y.O., Dodd, P.R., Tiwari, G.R., Harris, R.A., Mayfield, R.D., 2011. Up-regulation of MicroRNAs in brain of human alcoholics. Alcohol. Clin. Exp. Res. 35, 1928–1937. https://doi.org/10.1111/j.1530-0277.2011.01544.x.
Lind, P.A., Eriksson, C., Wilhelmsen, K.C., 2008. The role of aldehyde dehydrogenase-1 (ALDH1A1) polymorphisms in harmful alcohol consumption in a Finnish population. Hum. Genomics 3, 24. https://doi.org/10.1186/1479-7364-3-1-24.
Lischinsky, J.E., Lin, D., 2020. Neural mechanisms of aggression across species. Nat. Neurosci. 23, 1317–1328. https://doi.org/10.1038/s41593-020-00715-2.
MacDonald, M., H.D.C.R.G. (HDCRG), 1993. A novel gene containing a trinucleotide repeat that is expanded and unstable on Huntington's disease chromosomes. Cell 72, 971–983. https://doi.org/10.1016/0092-8674(93)90585-E.
Maltese, M., Stanic, J., Tassone, A., Sciamanna, G., Ponterio, G., Vanni, V., Martella, G., Imbriani, P., Bonsi, P., Mercuri, N.B., Gardoni, F., Pisani, A., 2018. Early structural and functional plasticity alterations in a susceptibility period of DYT1 dystonia mouse striatum. Elife 7. https://doi.org/10.7554/eLife.33331.
Mangiarini, L., Sathasivam, K., Seller, M., Cozens, B., Harper, A., Hetherington, C., Lawton, M., Trottier, Y., Lehrach, H., Davies, S.W., Bates, G.P., 1996. Exon 1 of the HD gene with an expanded CAG repeat is sufficient to cause a progressive neurological phenotype in transgenic mice. Cell 87, 493–506. https://doi.org/10.1016/S0092-8674(00)81369-0.
Matsuoka, Y., Furuyashiki, T., Yamada, K., Nagai, T., Bito, H., Tanaka, Y., Kitaoka, S., Ushikubi, F., Nabeshima, T., Narumiya, S., 2005. Prostaglandin E receptor EP1 controls impulsive behavior under stress. Proc. Natl. Acad. Sci. 102, 16066–16071. https://doi.org/10.1073/pnas.0504908102.
McGarry, A., McDermott, M.P., Kieburtz, K., Fung, W.L.A., McCusker, E., Peng, J., de Blieck, E.A., Cudkowicz, M., 2019. Risk factors for suicidality in Huntington disease. Neurology 92, e1643–e1651. https://doi.org/10.1212/WNL.0000000000007244.
Medvedeva, V.P., Rieger, M.A., Vieth, B., Mombereau, C., Ziegenhain, C., Ghosh, T., Cressant, A., Enard, W., Granon, S., Dougherty, J.D., Groszer, M., 2019. Altered social behavior in mice carrying a cortical Foxp2 deletion. Hum. Mol. Genet. 28, 701–717. https://doi.org/10.1093/hmg/ddy372.
Nakamura, F., Kumeta, K., Hida, T., Isono, T., Nakayama, Y., Kuramata-Matsuoka, E., Yamashita, N., Uchida, Y., Ogura, K., Gengyo-Ando, K., Mitani, S., Ogino, T., Goshima, Y., 2014. Amino- and carboxyl-terminal domains of Filamin-a interact with CRMP1 to mediate Sema3A signalling. Nat. Commun. 5, 5325. https://doi.org/10.1038/ncomms6325.
Nance, M.A., Sanders, G., 1996. Characteristics of individuals with Huntington disease in long-term care. Mov. Disord. 11, 542–548. https://doi.org/10.1002/mds.870110509.
Penzes, P., Cahill, M.E., 2012. Deconstructing signal transduction pathways that regulate the actin cytoskeleton in dendritic spines. Cytoskeleton 69, 426–441. https://doi.org/10.1002/cm.21015.
Pflanz, S., Besson, J.A.O., Ebmeier, K.P., Simpson, S., 1991. The clinical manifestation of mental disorder in Huntington's disease: a retrospective case record study of disease progression. Acta Psychiatr. Scand. 83, 53–60. https://doi.org/10.1111/j.1600-0447.1991.tb05511.x.
Pla, P., Orvoen, S., Saudou, F., David, D.J., Humbert, S., 2014. Mood disorders in Huntington's disease: from behavior to cellular and molecular mechanisms. Front. Behav. Neurosci. 8 https://doi.org/10.3389/fnbeh.2014.00135.
Puigdellívol, M., Cherubini, M., Brito, V., Giralt, A., Suelves, N., Ballesteros, J., Zamora-Moratalla, A., Martín, E.D., Eipper, B.A., Alberch, J., Ginés, S., 2015. A role for Kalirin-7 in corticostriatal synaptic dysfunction in Huntington's disease. Hum. Mol. Genet. 24, 7265–7285. https://doi.org/10.1093/hmg/ddv426.
Renoir, T., Zajac, M.S., Du, X., Pang, T.Y., Leang, L., Chevarin, C., Lanfumey, L., Hannan, A.J., 2011. Sexually dimorphic serotonergic dysfunction in a mouse model of Huntington's disease and depression. PLoS One 6, e22133. https://doi.org/10.1371/journal.pone.0022133.
Ribasés, M., Sánchez-Mora, C., Ramos-Quiroga, J.A., Bosch, R., Gómez, N., Nogueira, M., Corrales, M., Palomar, G., Jacob, C.P., Gross-Lesch, S., Kreiker, S., Reif, A., Lesch, K. P., Cormand, B., Casas, M., Bayés, M., 2012. An association study of sequence variants in the forkhead box P2 (FOXP2) gene and adulthood attention-deficit/hyperactivity disorder in two European samples. Psychiatr. Genet. 22, 155–160. https://doi.org/10.1097/YPG.0b013e328353957e.
Sanjuán, J., Tolosa, A., González, J.C., Aguilar, E.J., Pérez-Tur, J., Nájera, C., Moltó, M. D., Frutos, R. de, 2006. Association between FOXP2 polymorphisms and schizophrenia with auditory hallucinations. Psychiatr. Genet. 16, 67–72. doi: https://doi.org/10.1097/01.ypg.0000185029.35558.bb.
Shelbourne, P.F., Killeen, N., Hevner, R.F., Johnston, H.M., Tecott, L., Lewandoski, M., Ennis, M., Ramirez, L., Li, Z., Iannicola, C., Littman, D.R., Myers, R.M., 1999. A Huntington's disease CAG expansion at the murine Hdh locus is unstable and associated with Behavioural abnormalities in mice. Hum. Mol. Genet. 8, 763–774. https://doi.org/10.1093/hmg/8.5.763.
Sia, G.M., Clem, R.L., Huganir, R.L., 2013. The human language–associated gene SRPX2 regulates synapse formation and vocalization in mice. Science (80-.) 342, 987–991. https://doi.org/10.1126/science.1245079.
Solberg, O.K., Filkuková, P., Frich, J.C., Feragen, K.J.B., 2018. Age at death and causes of death in patients with Huntington disease in Norway in 1986–2015. J. Huntingtons. Dis. 7, 77–86. https://doi.org/10.3233/JHD-170270.
Soler Artigas, M., Sánchez-Mora, C., Rovira, P., Richarte, V., Garcia-Martínez, I., Pagerols, M., Demontis, D., Stringer, S., Vink, J.M., Børglum, A.D., Neale, B.M., Franke, B., Faraone, S.V., Casas, M., Ramos-Quiroga, J.A., Ribasés, M., 2020. Attention-deficit/hyperactivity disorder and lifetime cannabis use: genetic overlap and causality. Mol. Psychiatry 25, 2493–2503. https://doi.org/10.1038/s41380-018-0339-3.
Spires, T.L., Grote, H.E., Garry, S., Cordery, P.M., Van Dellen, A., Blakemore, C., Hannan, A.J., 2004. Dendritic spine pathology and deficits in experience-dependent dendritic plasticity in R6/1 Huntington's disease transgenic mice. Eur. J. Neurosci. 19, 2799–2807. https://doi.org/10.1111/j.0953-816X.2004.03374.x.
Thompson, J.C., Harris, J., Sollom, A.C., Stopford, C.L., Howard, E., Snowden, J.S., Craufurd, D., 2012. Longitudinal evaluation of neuropsychiatric symptoms in Huntington's disease. J. Neuropsychiatry Clin. Neurosci. 24, 53–60. https://doi.org/10.1176/appi.neuropsych.11030057.
Tolosa, A., Sanjuán, J., Dagnall, A.M., Moltó, M.D., Herrero, N., de Frutos, R., 2010. FOXP2 gene and language impairment in schizophrenia: association and epigenetic studies. BMC Med. Genet. 11, 114. https://doi.org/10.1186/1471-2350-11-114.
Walker, F.O., 2007. Huntington's disease. Lancet 369, 218–228. https://doi.org/10.1016/S0140-6736(07)60111-1.
Wong, E.H.M., So, H.-C., Li, M., Wang, Q., Butler, A.W., Paul, B., Wu, H.-M., Hui, T.C.K., Choi, S.-C., So, M.-T., Garcia-Barcelo, M.-M., McAlonan, G.M., Chen, E.Y.H., Cheung, E.F.C., Chan, R.C.K., Purcell, S.M., Cherny, S.S., Chen, R.R.L., Li, T., Sham, P.-C., 2014. Common variants on Xq28 conferring risk of schizophrenia in Han Chinese. Schizophr. Bull. 40, 777–786. https://doi.org/10.1093/schbul/sbt104.
Wood, N.I., Morton, A.J., 2015. Social behaviour is impaired in the R6/2 mouse model of Huntington's disease. J. Huntingtons. Dis. 4, 61–73.